Ceramics International xxx (xxxx) 1–8

Contents lists available at ScienceDirect

Ceramics International

journal homepage: www.elsevier.com/locate/ceramint

Optimization of the ceramic ink used in Direct Ink Writing through rheological properties characterization of zirconia-based ceramic materials

M. Yarahmadi [a, b], P. Barcelona [c], G. Fargas [a, b], E. Xuriguera [c], J.J. Roa [a, b, *]

[a] CIEFMA-Department of Materials Science, Universitat Politècnica de Catalunya, Barcelona-Tech, Campus Diagonal Besos-EEBE, Barcelona, 08019, Spain
[b] Centre for Research in Multiscale Engineering of Barcelona, Universitat Politècnica de Catalunya, Barcelona-Tech, Campus Diagonal Besos-EEBE, Barcelona, 08019, Spain
[c] Department of Materials Science and Physical Chemistry, Universitat de Barcelona, Martí i Franquès, 1-11, 08028, Barcelona, Spain

ARTICLE INFO

Keywords:
Zirconia-based ceramic materials
Rheological properties
Feedstock characterization

ABSTRACT

Understanding and optimization the rheological properties characterization of zirconia (ZrO_2) based ceramics inks is critical for optimizing the production of Direct Ink Writing (DIW) components to achieve complex structures with similar properties as those obtained by using the traditional processing routes. In this work, ZrO_2 based ceramic materials with different yttrium contents (3 and 8 mol %) were designed and produced by DIW to determine the most suitable ceramic ink composition in terms of the rheological properties (e.g. flow curves, viscosity, loss modulus G′, storage modulus G″, etc.) to design new components. Different ceramic inks with charges up to 75 wt % were prepared and characterized. A systematic study of the feedstock, as well as the different ceramic inks, was performed to determine the optimal ceramic charge. This characterization evidences that rheological properties of zirconia based ceramic inks are influenced by the particle size and amount of ceramic content. Furthermore, the rheological study highlights that the ZrO_2 inks present a Non-Newtonian behavior depending on the ceramic content. Results revealed that the yttrium content affects the flow properties of ZrO_2 suspensions in such a way that, higher shear rate was required to make the suspensions flow at increasing the amount of powder. It was also found that the best rheological properties corresponded to 73 and 70% for the 3Y- and 8Y–ZrO_2 of ceramic charge, respectively.

1. Introduction

Zirconia (ZrO_2), due to its excellent mechanical properties, holds a unique place amongst other ceramic oxides [1]. It can be used as a structural bioceramic by doping the material with secondary phases (i.e. yttrium oxide, calcium oxide, etc.) in order to stabilize the tetragonal phase at room temperature. In this regard, 3 or 8 mol % of yttrium oxide (Y_2O_3) are widely employed as stabilizers leading to stress-inducing tetragonal (*t*-) → monoclinic (*m*-) phase transformation, a mechanism also known as martensitic transformation [2,3]. In this sense, ZrO_2 based ceramic materials have multiple commercial applications depending on the Y_2O_3 content [4,5]; like electrolytes in solid oxide fuel cells by using 8 mol.% Y_2O_3–ZrO_2 (8Y–ZrO_2), dental implants and prosthesis mainly using 3 mol % Y_2O_3–ZrO_2 (3Y–ZrO_2), among other applications. Currently, the traditional processing routes used in these specimens provide specimens with different shapes as cylinders or even foams. On the other hand, parts produced by traditional routes are relatively large, and geometric complexity is a limitation in the cold isostatic (CIP) method [6,7]. However, these geometries are not necessarily optimal for the different types of applications in several sectors.

In this sense, as a rapidly growing industry with an expanding opportunity set, Additive Manufacturing (AM) has applications in numerous markets, ranging from aerospace to energy [6]. The combination of the limitless potential offered by this technology and the ever-decreasing cost of the printing machines supports the increasing popularity of AM in the energy industry [7]. In this context, solid freeform fabrication has become one of the key manufacturing techniques leading to the design and development of complex shapes. This technology includes a wide range of methodologies [8], such as powder bed fusion (e.g. selective laser melting [9,10]), sheet lamination (e.g. laminated object manufacturing [11]), vat photopolymerization (e.g. stereolithography [12]), material extrusion (fused deposition of ceramics [13–15]), binder jetting [16–18], material jetting (e.g. ink-jet printing [19,20] and direct-ink-writing (DIW) [21]. In particular, material extrusion by DIW is of special interest due to its ability to produce space filling and spanning structures as well as to provide relatively easy access to multi-

* Corresponding author. CIEFMA-Department of Materials Science, Universitat Politècnica de Catalunya, Barcelona-Tech, Campus Diagonal Besos-EEBE, Barcelona, 08019, Spain.
E-mail address: joan.josep.roa@upc.edu (J.J. Roa).

https://doi.org/10.1016/j.ceramint.2021.11.013
Received 6 August 2021; Received in revised form 11 October 2021; Accepted 2 November 2021

material AM. The first step is to design the solid object using computer modeling software such as Computer-Aided Design (CAD). In this sense, the final geometry can be chosen arbitrarily without the need to modify the rest of the manufacturing process which allows expanding opportunities within the scientific and industrial field. The DIW technology [22] can be considered as a desirable alternative for the industry of the future that allows better control of topology and/or geometry. This technology leads to build complex geometries layer-by-layer using a bottom-up methodology. The rheological properties are the main key parameter by using the DIW technology in order to implement complex and dense ceramic structures. In this sense, from one ceramic ink to another mainly depends on several experimental parameters which can modify the rheological properties such as particle size, pH of suspending media, type and amount of added dispersing agents, among others [23–26].

Following the above ideas, it is clear that the use of the DIW technology to develop complex structures which emerge as a suitable approach for the demanding applications of ZrO_2 based ceramic materials. It is well known that the DIW technology imposes strict requirements on their printability which is strongly correlated with the rheological properties of the ceramic inks. In this sense, the ceramic inks not only must flow through the nozzle but also resist deformation immediately after being printed. This research aims to optimize in terms of the rheological properties of the ceramic ink formulation in terms of the Y_2O_3 content for ZrO_2 based ceramic materials to enhance their printability.

2. Experimental procedure

2.1. Materials

The commercial ceramic feedstock powders used in the preparation of the ceramic inks were 3 mol % Y_2O_3 - and 8 mol % Y_2O_3–ZrO_2 also labelled as 3Y–ZrO_2 and 8Y–ZrO_2, respectively, from TOSOH Corporation and Pluronic® F-127 (Sigma Aldrich, Germany) were used to prepare the gelling agent.

2.2. Ceramic inks

A dual asymmetric centrifugal mixer (SpeedMixer, DAC 150.1 FVZ-k) was employed to mix the gelling agent (Pluronic® F-127 + distilled water) and the ceramic charge (3Y- and 8Y–ZrO_2) for 30 s, with different ratios of ceramic charges (CC)/gelling agent in order to optimize the ceramic ink in terms of printability as follows: 75/25, 73/27, 71/29 and 72/28, 70/30, 68/32 for the 3Y- and 8Y–ZrO_2, respectively.

The ceramic ink preparation was done in two different steps: (1) initially, the gelling agent was prepared from a solution of 25 wt% of Pluronic® F-125 in 75 wt % of distilled water. Subsequently, the mixture was cooled down at 4 °C for 24 h to release the defects generated during the mixing process (i.e. bubbles) and (2) afterward, the ceramic powder was added to this solution to prepare the desired ceramic ink with different ratios between gelling agent/ceramic charge as described above.

2.3. Feedstock characterization

The morphology of the feedstock was characterized by field-emission scanning electron microscopy (FESEM, Jeol 7001F). Prior the particle size measurement, the feedstock was dispersed on distilled water and subsequently measured by laser diffraction analysis (Malvern, Mastersizer 3000 Hydro EV).

X-Ray diffraction (XRD, 2θ angle: 25° to 75°) analyses were carried out on a Philips MRD using Cu $K\alpha_1$ (40 kV and 30 mA) radiation. The spectra were obtained at a scan rate of 10 s·step^{-1} and with a constant scan size of 0.017°.

2.4. Rheological properties

Rheological properties of the gelling agent and ceramic inks investigated in this manuscript were characterized at room temperature in a Thermo Scientific HAAKE MARS III rheometer (Thermo-Fisher Scientific, USA) with a 20 mm serrated parallel plate geometry at 25 °C. Rheological parameters were determined by rotational measurements in controlled shear rate mode increasing shear rate from 0.1 s^{-1} to 200 s^{-1} logarithmically and decreasing the shear rate to the initial value in the same form. Viscoelastic behavior was evaluated by oscillatory measurements. G′ and G″ were evaluated increasing the shear strain from 10 to 10000 Pa at a constant 1 Hz frequency. G′ and G″ were determined from the hydrogel at different frequencies from 0.001 to 100 Hz at constant 100 Pa of shear strain. Viscoelastic suspensions are characterized by their complex shear modulus (G^*) as follows [27]:

$$G^* = G' + i{\cdot}G'' \quad (1)$$

where G^* is composed of the real component (G'), and an imaginary component (G''). G' represents the energy stored in the elastic structure while the G'' characterizes the amount of energy dissipated and/or the viscous part of the specimen.

3. Results and discussion

3.1. Feedstock characterization

The XRD patterns for the ZrO_2 based ceramic feedstocks investigated here with different Y_2O_3 content (3Y- and 8Y–ZrO_2) recorded in a wide range of Bragg angle 2θ (0° ≤ 2θ ≤ 100°) are depicted in Fig. 1. All the observed diffraction peaks can be indexed with the main constitutive phases present in the material; tetragonal (*t-*), monoclinic (*m-*), and cubic (*c-*) ZrO_2 phases. For 3Y–ZrO_2 (black spectra) it is possible to observe that the asymmetrical broadening of the $(111)_t$ peak at around 30°. On the other hand, at 34.64° and 35.22° corresponds to the $(002)_t$ and $(200)_t$ planes which correspond to the tetragonal doublet in agreement with [28]. Furthermore, the XRD spectra for the 3Y–ZrO_2 shows the presence of the *m*-phase at 20 and around 35°. On the other hand, the 8Y–ZrO_2 spectra shows the existence of the *c*-phase in agreement with those reported in Refs. [29,30]. Fig. 2 shows the particle morphology (left side) and the particle size distribution (right side) for the 3Y- and 8Y–ZrO_2 feedstocks. SEM micrographs of the different feedstocks

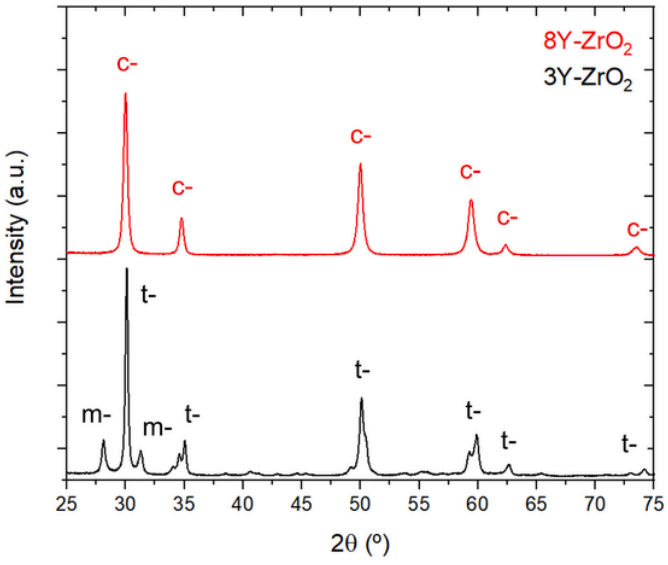

Fig. 1. XRD spectra of the 3Y- and 8Y–ZrO_2 feedstocks. *t-*, *m-* and *c*-present in the graph denotes the tetragonal, monoclinic and cubic phases, respectively.

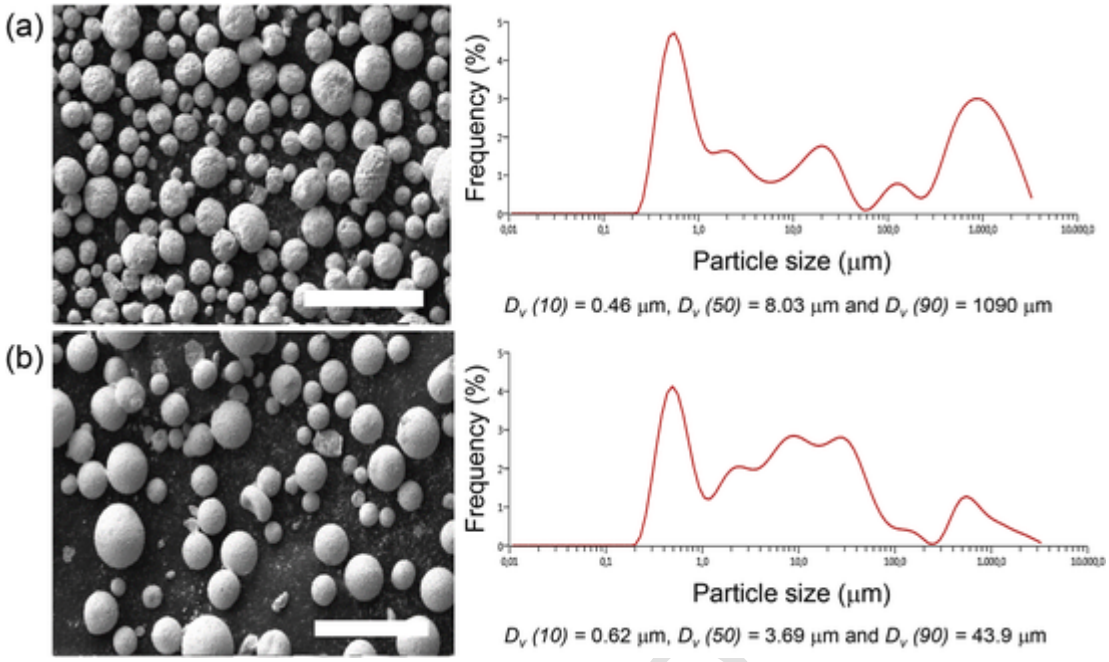

Fig. 2. SEM micrographs and particle size distribution of the investigated feedstock: (a) 3Y- and (b) 8Y–ZrO_2. SEM scale bar: 100 μm.

(see Fig. 2, left side) exhibit a quasi-spherical bimodal shape distribution. Moreover, they have no difference in morphological structure and they tend to agglomerate as depicted in Fig. 3. The particle size distribution for both investigated feedstocks presents a multi-modal particle size distribution. 3Y–ZrO_2 feedstock exhibits a bimodal particle size distribution of fine and coarse particles at around 0.46 and 8.03 μm, respectively, being the coarse particle size distribution agglomerates. A similar trend is presented for the 8Y–ZrO_2 with a mean particle size smaller than those for the 3Y–ZrO_2.

3.2. Rheological properties

Prior to validating the suitability of the ceramic inks, rheological measurements were initially performed on the gelling agent (Pluronic® F-127/distilled water with the following ratio: 25/75 wt %) to determine the physical properties which may be useful to provide a framework for the formulation of the correct ink as depicted in Fig. 3.

Fig. 3a exhibits G′ and the G″ as a function of the shear stress applied from oscillatory stress sweep. A different behavior was found depending on the intensity of the stress. At low shear stress, G′ and G″ values for the gelling agent remained constant and parallel within the linear viscoelastic region (LVR). Furthermore, as shear stress increased, G′ decreased indicating a breakdown of the internal structure of the gelling agent in agreement with Refs. [27,31]. Furthermore, G″ showed a slight increase before crossover with G'. Above the cross-over stress, G″ exceeded G′ indicating then that transition is predominantly from solid to liquid behavior. Fig. 3b shows the viscosity evolution as a function of the shear rate (black curve), which decreases linearly. This trend indicates that the gelling agent presents a shear thinning behavior in agreement with previous studies [32,33]. In this sense, this trend follows a non-Newtonian fluid behavior. On the other hand, at a high shear rate, the breakup happens faster than the deformation, so there is less resistance to flow (see the red curve in Fig. 3b). In order to evaluate the gel behavior, the G′ and G″ have been measured throughout the frequency range as shown in Fig. 3c. As it is depicted in Fig. 3c, G′ and G″ presents values higher than 10^3Pa at low frequencies (0.001 Hz), highlighting the structural stability of the gelling agent as a dispersion matrix. In this sense, it is well known that adding ceramic charge to the gelling agent this trend will be higher than the one for the gelling agent. From the aforementioned information, the stability of the ceramic ink has not been investigated due to the G′ and G″ as a function of the frequency will present values higher than for the gelling agent.

It is well established, that an ink suitable for DIW must be easy to flow through a nozzle, but they must resist deformation after printing. In this regard, it may keep in mind that the rheological properties are a key parameter to take into consideration. In this regard, inks suitable for robocasting must be easy to extrude through the nozzle and cohesive enough to hold its shape after printing process. In this sense, the three different ceramic charges per specimen have been investigated; 71, 73 and 75% and 68, 70 and 72% for 3Y- and 8Y–ZrO_2, respectively. Fig. 4 shows G′ and G″ as a function of the shear strain applied from oscillatory stress sweep. From this representation, at least two different parameters can be extracted, describing this yield phenomenon: at the end of the LVR region, meaning G′ dropping at least by more than 10% of the plateau value, and also the intersection between G′ and G″ and known as the yield stress, τ_y [34]. As it is presented in this representation, at low shear stress, G′ and G″ values for the ceramic ink remained constant and parallel within the LVR, being the G′ greater than G″ and denoting that at this region the ceramic ink is slightly structure and presents a solid-like behavior. Furthermore, as shear stress increased, G′ decreased indicating a breakdown of the internal structure of the material. As it is evident, the ceramic ink, G″ showed a slight increase before crossover with G'. Above the cross-over stress, G″ exceeded G′ indicating then that transition is predominantly from solid to liquid behavior. Finally, the cross-over point where *G″* becomes larger than *G′* - also known as the flow stress and represented as τ_y - is the moment where the applied mechanical force overtakes the molecular or inter particles forces and the material starts to flow. As can be seen in Fig. 4, either the ceramic charge of the ceramic ink increases and/or the Y content increases, the G′, G″ and τ_y increases. This means that more force is required in order to lead the ceramic ink flow through the nozzle. Based on the rheology characteristics, the minimum τ_y to extrude the ceramic inks in order to the geometry and the structural stability of the shaped object after the DIW project is around 73 and 70% of ceramic charge for the 3Y- and 8Y–ZrO_2, respectively. The main rheological properties extracted for the gelling agent as well as for the ceramic inks investigated here are summarized in Table 1. Furthermore, the minimum τ_y to ex-

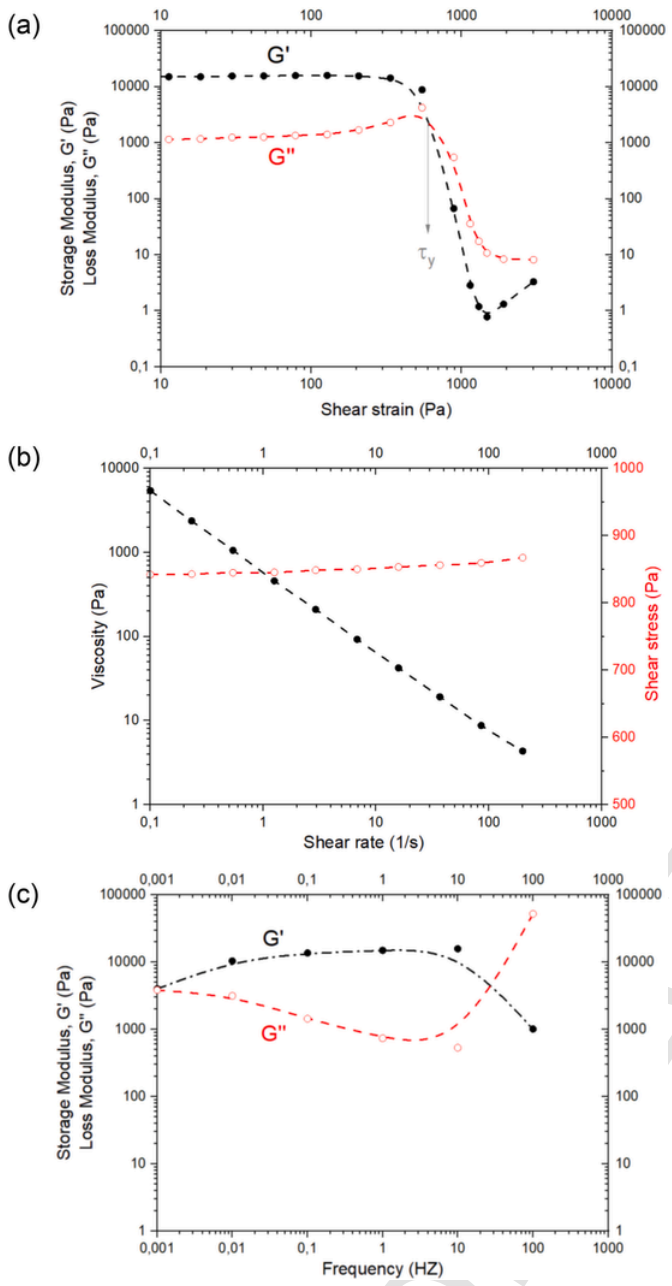

Fig. 3. Rheological properties for the gelling agent in log-log representation: (a) shear modulus vs. shear strain amplitude, (b) viscosity as a function of shear rate, and (c) shear modulus as a function of frequency.

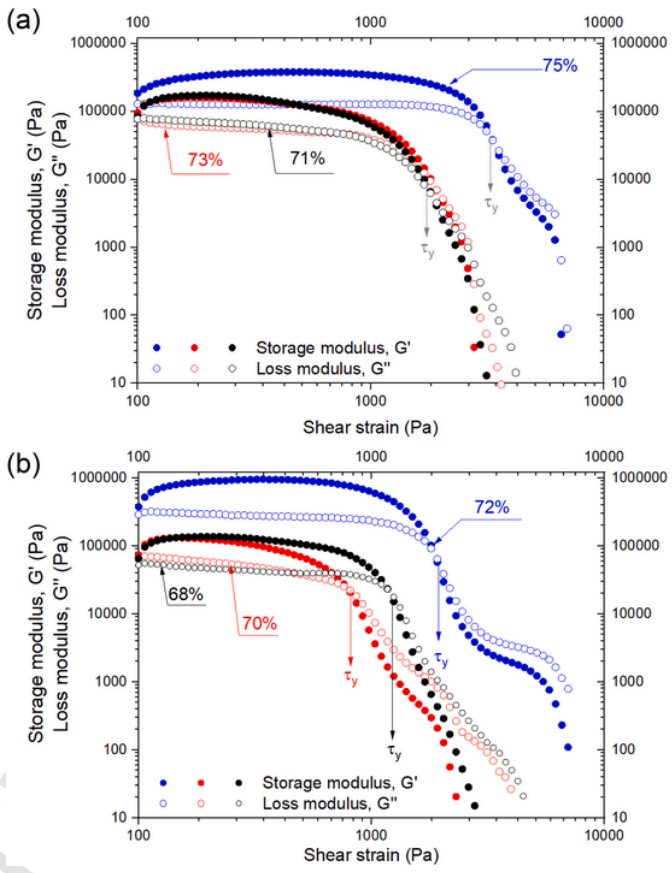

Fig. 4. Storage and loss modulus as a function of the shear strain for the different ceramic inks investigated here for a) 3Y- and b) 8Y–ZrO_2.

Table 1
Summary of the main rheological properties for the gelling agent as well as for the ceramic ink. Includes the data for all the ceramic inks investigated that appear in Figs. 5 and 6.

Sample	Viscosity at 100 s^{-1} shear rate (Pa) $\cdot 10^{-3}$	Yield stress (τ_y, Pa)	G* al LVR zone (Pa)$\cdot 10^{-3}$
Hydrogel	9	550	10 ± 7
3Y – 73%	6395	1439	120 ± 73
8Y – 70%	14499	2336	174 ± 90

trude the ceramic inks are around 1439 and 2336 Pa for the 3Y- and 8Y–ZrO_2, respectively.

Initially, in Fig. 5 it is possible to see the effect of the Y content for the optimized ceramic inks in terms of viscosity and shear stress for each ceramic ink investigated here as a function of the shear rate. As it is depicted, as the Y content increases, both trends present higher values. At low shear rates, the viscosity presents irregular changes, which proves that the ceramic charge investigated in this manuscript does not make the ink a steady flow. Furthermore, viscosity decreases when the shear rate increases reaching a stable state at a shear rate above 10 and 25 s^{-1} for 3Y–ZrO_2 (73% of ceramic charge) and 8Y–ZrO_2 (70% of ceramic charge), respectively. Furthermore, the ceramic inks present a shear thinning behavior following a step change in applied shear in fair agreement with the trend presented in Ref. [27]. In this representation, a sudden drop in viscosity is evident due to the disruption and breakdown of the network under shear stress [35]. Furthermore, when the dynamic viscosity linearly decreases as the shear rate increases, which means that the ceramic inks remain stable without any deformation after the DIW process in agreement with Refs. [36,37]. Non-hysteresis loop for both ceramic inks is visible in Fig. 5, which shows that the ceramic inks do not present a thixotropic behavior and at the same time the ceramic ink keeps the 3D printing structure after the DIW process in agreement with [38]. The obtained results indicate that the Y content affects the flow properties of ZrO_2 ceramic ink, improving the extrudability properties at high shear rates. At lower shear rates, viscosity linearly increases, and ceramic inks recover their initial state. At a high shear rate, the breakup happens faster than the reformation, so there is less resistance to flow [39]. The viscosity linearly decreases with time as the gelling structure is broken down until an equilibrium viscosity is reached. In this regard, and from the data presented in Fig. 4, the ceramic inks investigated here a suitable to be used for the DIW technology due to they retain the shape after each filament is deposited, which corresponds to a quick viscosity recovery when no shear stress is applied in agreement with Ref. [40].

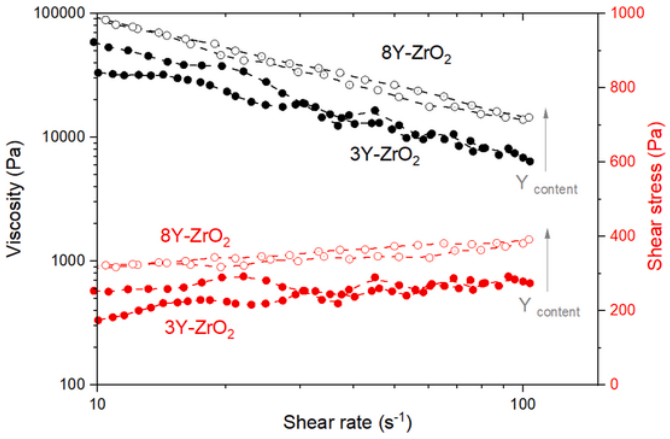

Fig. 5. Log-plot evolution of the viscosity and shear stress for the optimized ZrO_2 based ceramic materials (73 and 70 wt % for the 3Y- and 8Y–ZrO_2, respectively) with different Y content vs shear rate. Go and back correspond with the lower and upper curves, respectively.

Fig. 6a represents the values for G′ and G″ against shear strain for the gelling agent as well as for the two optimized ceramic inks. As it is evident, adding the ceramic charge into the gelling agent, the G′, G″ as well as the τ_y considerably increases. This effect can be attributed to the formation of a stiff network of particle interactions. The ceramic inks show a LVR at strains below 5–8%. On the other hand, τ_y takes place at 15–25% for the ceramic inks while it takes place at 50% of the shear strain applied for the gelling agents. These results confirm that both ceramic inks can have appropriate rheology to be used to 3D printing ceramic components by using the DIW technology as summarized in Table 1. As it is evident in this table as well as in Fig. 6a, the τ_y increases with the Y content. This trend can be attributed to the fact that the flow of the hydrogel is constricted by the presence of ceramic particles that share some of the load. In this sense, larger overall stress is required to instigate flow. On the other hand, by plotting the complex modulus (G^*) or the phase angle (δ) as a function of stress amplitude, exists a point where the trend loses the linearity that defines the limit of the linear viscoelastic region as shown in Fig. 6b.

3.3. Relationship between rheological properties vs. extrusion

The flow behavior of these ceramic inks investigated along this research can often be approximated by the Herschel-Bulkley model [41]. This has been found to be useful for describing the flow of robocasting inks and describes ideal non-Newtonian fluids which do not flow below certain stress (the yield stress). When they are stressed above their yield stress, they exhibit shear thinning behavior, such that their viscosity decreases greatly as shear rate increases [41]. They can be mathematically described by the Herschel-Bulkley equation [27,41];

$$\tau = \tau_y + K\dot{\gamma}^{(n)} \quad (1)$$

where τ is the applied shear stress, τ_y is the yield stress, $\dot{\gamma}$ is the shear rate, n is the shear thinning exponent and K is the viscosity parameter. For robocasting and in particular for the DIW, a low value of n is desirable such that extrusion pressures are reasonably low and to aid mixing. This model describes materials with viscosity that varies with shear rate, and exhibit a yield stress ($\tau_y > 0$). When $n<1$ viscosity will decrease with shear rate [27,41]]. This phenomenon is known as shear thinning or pseudo-plasticity, and is a very common rheological behavior. Materials where $n = 1$ and $\tau_y = 0$ are Newtonian fluids, while materials where $n>1$ are shear thickening, meaning their viscosity increases with shear rate [27,38,41]]. Within the aforementioned information, Fig. 7 shows data of calculating the viscosity parameter (K) and shear thinning coefficient (n) of 3Y–ZrO_2 and 8Y–ZrO_2 inks under the best rheological properties. As the yield stress τ_y is the yield stress with the flow point in Herschel-Bulkley model. The slopes are 0.39 and 0.82 which means that they are the values of (n) for 3Y-73% and 8Y-70% ink, respectively. The intercepts are 5.01 and 2.75 which are equal to ln (K), so the value of K are 149.9 Pa.s^n for 3Y-73% and 262.4 Pa.s^n for 8Y-70% ink, respectively. All of our inks and hydrogel exhibited a yield stress ($\tau_y > 0$) and were shear thinning at stresses above the yield stress ($0 < n < 1$).

4. Conclusions

A systematic study to determine the optimal formulation of a ceramic ink with two different yttria content for DIW technology is conducted. Key parameters studied are ceramic content and rheological properties. The following conclusions can be drawn:

(1) The rheology and processing ability of the inks depends on feedstock content and particle-size distribution.
(2) The viscosity of the different examined decreases when the shear rate increases. This behavior highlights that the ceramic inks present a shear thinning effect. This means that there is a great resistance to flow at a low shear rate and this behavior is enhanced by the addition of ceramic charge and high connection between the particles.
(3) Furthermore, the shear thinning behavior is preferable as it allows the paste to be extruded through smaller nozzles at a lower pressure. As might be expected, at low shear rates, viscosity was found to increase with increasing yttrium content.
(4) The shear stress curve of the different ceramic inks showed the reversible behavior that means break down and build-up of microstructure due to the reversible disruption and breakdown of the gelling agent network under stress.
(5) Through rheological characterization, the optimal ceramic charge for the different investigated ceramic inks are 73 and 70% for the 3Y- and 8Y–ZrO_2, respectively. These inks present a pseudoplastic behavior.
(6) The optimized ceramic inks exhibited a similar trend as for the gelling agent but with the main investigated rheological properties (G′, G″, τ_y and η) slightly higher for the ceramic inks due to the addition of the 3Y- and 8Y–ZrO_2 charge into the gelling agent.

Declaration of competing interest

The authors declare that they have no known competing financial interests or personal relationships that could have appeared to influence the work reported in this paper.

Acknowledgments

This work has been partially funded by the EU Regional Development within the framework of the Operational FEDER of Catalonia 2014–2020 RIS3CAT-BASE3D. JJR is Serra Húnter fellow from Generalitat de Catalunya.

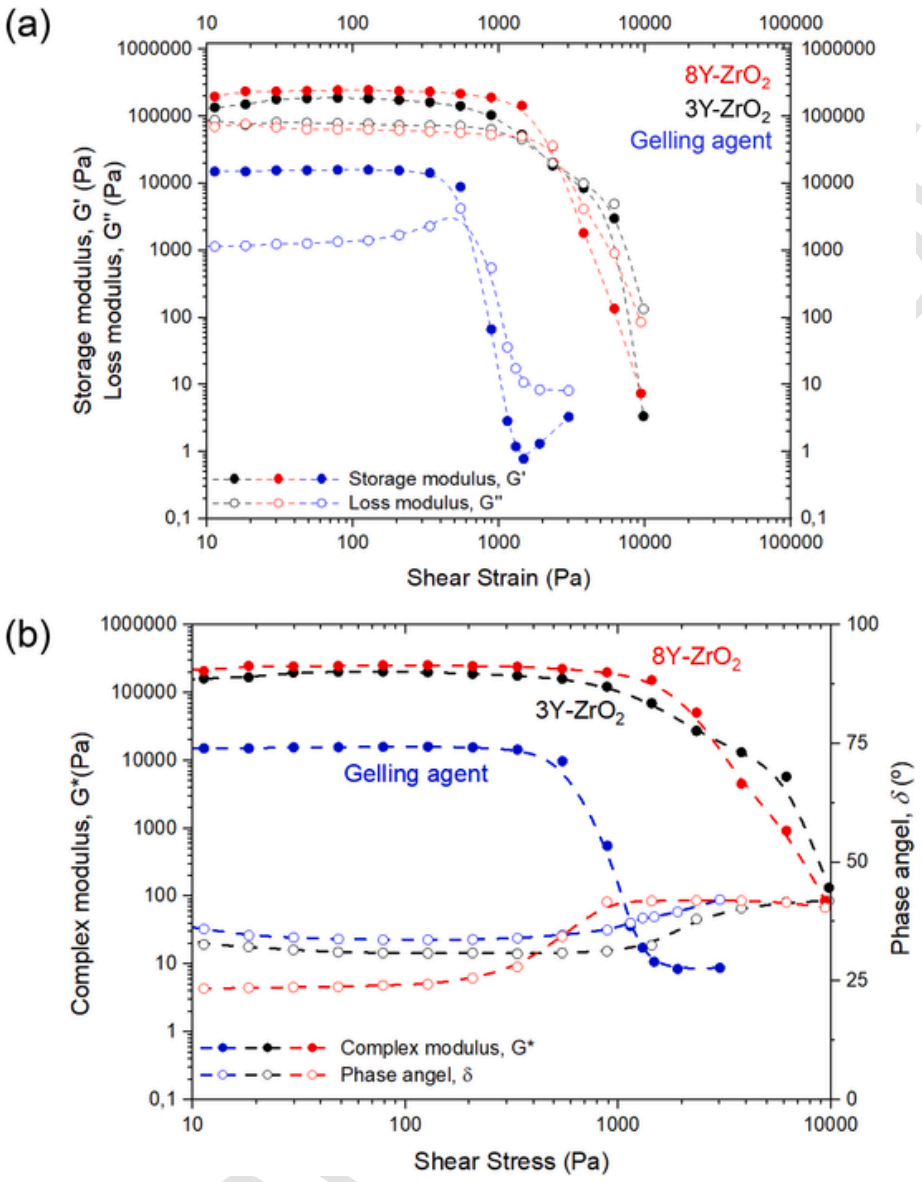

Fig. 6. (a) Shear and loss modulus vs shear strain amplitude for the gelling agents as well as for the optimized ceramic inks and (b) variation of the complex modulus (G^*) and phase angle (δ) as a function of the shear stress sweep test performed at a constant frequency of 1 Hz.

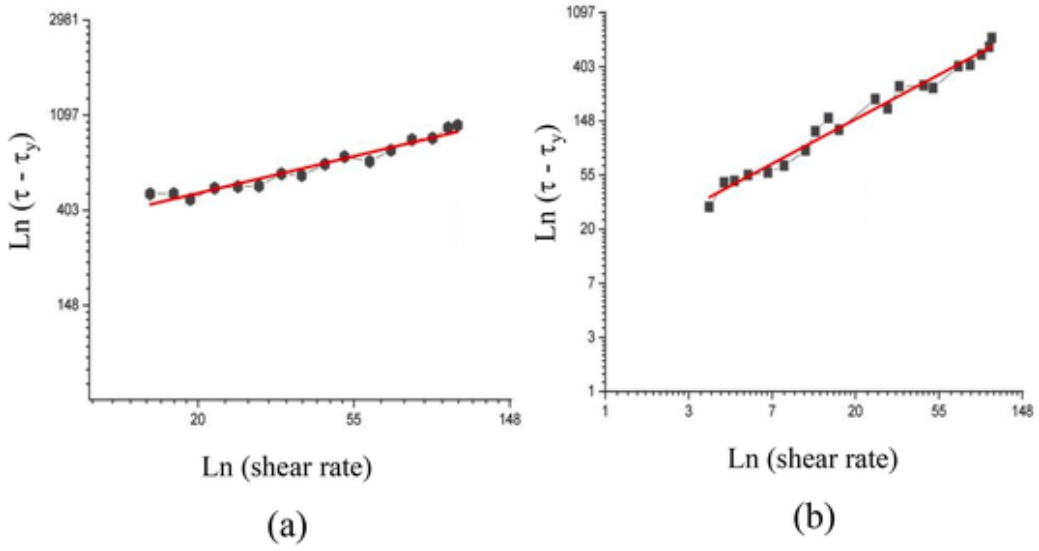

Fig. 7. Ln-plot calculation of K and n for (a) 3Y–ZrO2 (73 wt% of ceramic charge) and (b) 8Y–ZrO2 (70 wt% of ceramic charge). This representation has been conducted by using the data from Fig. 5.

References

[1] J. Chevalier, What future for zirconia as a biomaterial? Biomaterials 27 (4) (2006) 535–543.
[2] I. Denry, J.R. Kelly, State of the art of zirconia for dental applications, Dent. Mater. 24 (3) (2008) 299–307.
[3] P. Pittayachawan, Comparative Study of Physical Properties of Zirconia Based Dental Ceramics, Doctoral thesis. UCL (University College London), 2008, pp. 1–324.
[4] H. Yamaguchi, S. Ino, N. Hamano, S. Okada, T. Teranaka, Examination of bond strength and mechanical properties of Y-TZP zirconia ceramics with different surface modifications, Dent. Mater. 31 (3) (2012) 472–480.
[5] D.R.R. Lazar, M. C Bottino, M. Ozcan, L. Felipe Valandro, R. Amaral, V. Ussui, A.H.A. Bressiani, Y-TZP ceramic processing from coprecipitated powders: a comparative study with three commercial dental ceramics, Dent. Mater. 24 (12) (2008) 1676–1685.
[6] J.C. Ruiz-Morales, A. Tarancón, J. Canales-Vázquez, J. Méndez-Ramos, L. Hernández-Afonso, P. Acosta-Mora, J.R. Marín Rueda, R. Fernández-González, Three dimensional printing of components and functional devices for energy and environmental applications, Energy Environ. Sci. 10 (4) (2017) 846–859.
[7] K.S. Prakash, T. Nancharaih, V.V.S. Rao, Additive manufacturing techniques in manufacturing -an overview, Mater. Today Proc. 5 (2) (2018) 3873–3882.
[8] A. Martínez García, M. Monzón, R. Paz, Standards for Additive Manufacturing Technologies: Structure and Impact, Handbooks in Advanced Manufacturing, 2021, pp. 395–408 (Chapter 12).
[9] H.L. Marcus, J. Beaman, S.J.W. Barlow, D.L. Boumell, Solid freeform fabrication: powder processing, J. Am. Ceram. Soc. 69 (1990) 1030–1031.
[10] P.K. Subramanian, H.L. Marcus, Selective laser sintering of alumina using alumina binder, Mater. Manuf. Process. 10 (1995) 689–706.
[11] C. Griffin, D. Bautenbach, S. McMillin, Desktop manufacturing: LOM vs pressing, J. Am. Ceram. Soc. 73 (1994) 80–113.
[12] M.L. Griffith, J.W. Halloran, Freeform fabrication of ceramics via stereolithography, J. Am. Ceram. Soc. 79 (1996) 2601–2608.
[13] S.C. Danforth, Fused Deposition of Ceramics: a new technique for the rapid fabrication of ceramics components, Mater. Technol. 10 (1999) 144–146.
[14] M.K. Agarwala, V.R. Jamalabad, N.A. Langrana, A. Safari, P.J. Whalen, S.C. Danforth, Structural quality of parts processed by fused deposition, Rapid Prototyp. 2 (1996) 4–19.
[15] M.K. Agarwala, A. Bandyopadhyay, R.V. Weeren, A. Safari, S.C. Danforth, N.A. Langrana, V.R. Jamalabad, P.J. Whalen, FDC Rapid Fabrication of Structural Components, vol. 75, American Ceramic Society, 1996, pp. 60–66.
[16] E. Sachs, M. Cima, P. Williams, D. Brancazio, J. Cornie, Three dimensional printing, rapid tooling and prototypes directly from a CAD model, Eng. Indus. Trans. AMSE 114 (1992) 481–488.
[17] J. Grau, M. Cima, E. Sachs, Fabricating alumina molds for slip casting and 3-D printing, Ceram. Indus. 146 (1996) 22–27.
[18] J. Yoo, M. Dima, E. Sachs, S. Suresh, Fabrication and microstructural control of advanced ceramics components by three dimensional printing, Ceram. Eng. Sci. Proc. 16 (1995) 755–762.
[19] Q.F. Xiang, J.R.G. Evans, M.J. Edirisinghe, P.F. Blazdell, Solid freeforming of ceramics using a drop-on-demand jet printer, Eng. Manuf. 211 (1997) 211–214.
[20] W.D. Teng, M.J. Edirsinghe, Development of Continuous Direct Ink-Jet Printing of Ceramics, vol. 81, American ceramic society, 2005, pp. 169–173.
[21] A. M'Barki, L. Bocquet, A. Stevenson, Linking rheology and printability for dense and strong ceramics by direct ink writing, Sci. Rep. 7 (2017) 6017/1–6017/10.
[22] I. Gibson, D. Rosen, B. Stucker, Additive Manufacturing Technologies: 3D Printing, Rapid Prototyping, and Direct Digital Manufacturing, Springer-Verlag new york, 2020, pp. 23–51.
[23] A.K. Nikumbh, P.V. Adhyapak, Formation characterization and rheological properties of zirconia and ceria-stabilized zirconia, Sci. Res. (N. Y.) (2010) 694–706, 02.
[24] D. Sharma, A. Mukherjee, Essential parameters responsible for rheological assessment of concentrated dispersion:- A comprehensive review, Ceram. Process Res. 16 (2015) 690–704.
[25] E. Özkol, Rheological Characterization of Aqueous 3Y-TZP Inks Optimized for Direct Thermal Ink-Jet Printing of Ceramic Components, vol. 96, American Ceramic Society, 2013, pp. 1124–1130.
[26] M. Faes, H. Valkenaers, F. Vogeler, J. Vleugels, E. Ferraris, Extrusion-based 3D printing of ceramic components, Procedia CIRP 28 (2015) 76–81.
[27] E. Feilden, Additive Manufacturing of Ceramics and Ceramic Composites via Robocasting, Doctoral thesis. Department of Materials (Imperial College London), 2017, pp. 1–200.
[28] L. Melk, J. Mouzon, M. Turon, F. Akhtar, M.L. Antti, M. Anglada, Surface microstructural changes of spark plasma sintered zirconia after grinding and annealing, Ceram. Int. 42 (2016) 15610–15617.
[29] S.B. Martins, F. de O. Abi-Rached, G.L. Adabo, P. Baldissara, R.G. Fonseca, Influence of particle and air-abrasion moment on Y-TZP surface characterization and bond strength, Prosthodont 28 (2019) 271–278.
[30] K. Matsui, H. Yoshida, Y. Ikuhara, Grain-boundary structure and microstructure development mechanism in 2-8 mol% yttria-stabilized zirconia polycrystals, Acta Mater. 56 (2008) (2008) 1315–1325.
[31] B.J.E. Smay, G.M. Gratson, R.F. Shepherd, J.C. Iii, J.A. Lewis, Directed colloidal assembly of 3D periodic structures, Adv. Mater. 14 (2002) 1279–1283.
[32] J. Jiang, et al., Shear-induced layered structure of polymeric micelles by SANS shear-induced layered structure of polymeric micelles by SANS, Macromolecules 40 (2007) 4016–4022.
[33] R.K. Prud, G. Wu, D.K. Schneider, Structure and rheology studies of poly (oxyethylene - oxypropylene - oxyethylene) aqueous solution, Langmuir 12 (1996) 4651–4659.
[34] T.G. Mezger, The Rheology Handbook, 2014, pp. 1–298.
[35] V. Pouyafar, S.A. Sadough, An enhanced Herschel-Bulkley model for thixotropic flow behavior of semisolid steel alloys, Process Metall. Mater. Process. Sci. 44 (2013) 1304–1310.
[36] M. Callan, E. Jang, J. Kelly, K. Nguyen, C. Marmorat, M. Rafailovich, Characterization of pluronic F127 for the controlled drug release vancomycin in the spinal column, Undergrad. Chem. Eng. Res. 6 (2017) 1–136.
[37] O. Al, L. Goyos-ball, E. García-tuñón, E. Fernández, R. Díaz, Mechanical and Biological Evaluation of 3D Printed 10CeTZP, vol. 37, European Ceramic Society, 2017, pp. 3151–3158.

[38] E. Feilden, E.G.T. Blanca, F. Giuliani, E. Saiz, L. Vandeperre, Robocasting of Structural Ceramic Parts with Hydrogel Inks, vol. 36, Europian Ceramic Society, 2016, pp. 2525–2533.
[39] D. Megías-Alguacil, J.D.G. Durán, A.V. Delgado, Yield stress of concentrated zirconia suspensions: correlation with particle interactions, Colloid Interface Sci. 231 (2000) 74–83.
[40] M.P. Id, P. Colombo, Optimization and Characterization of Preceramic Inks for Direct Ink Writing of Ceramic Matrix Composite Structures, 2018, pp. 1–14.
[41] Q. Cai, *Robocasting of Complex Structural Ceramics,* PhD Thesis, Imperial Collage Longon, 2017, pp. 1–228.